ORGANOMETALLICS
Article
pubs.acs.org/Organometallics

Palladium and Platinum Acyl Complexes and Their Lewis Acid Adducts. Experimental and Computational Study of Thermodynamics and Bonding

Danmin Chen, Michael R. Gau, and Graham E. Dobereiner*

Department of Chemistry, Temple University, Philadelphia, Pennsylvania 19122, United States

S *Supporting Information*

ABSTRACT: The interactions of Pt and Pd acyl complexes with Lewis acids are investigated through experiment and computation. Variable-temperature NMR studies indicate BF_3 association with *trans*-$[(PPh_3)_2(CO)Pt(COCH_2Ph)][BAr^F_4]$ (**3**; BAr^F_4 = tetrakis(3,5-bis(trifluoromethyl)phenyl)borate) at 298 K is endergonic ($\Delta G° = 2.0$ kcal mol^{-1}) yet exothermic ($\Delta H° = -3.4$ kcal mol^{-1}), suggesting a Lewis basicity comparable to or greater than aldehydes and ketones. Despite the accelerating effect of Lewis acids in the formation of the Pd congener *trans*-$[(PPh_3)_2(CO)Pd(COCH_2Ph)][BAr^F_4]$ (**4**), no evidence for adduct formation was obtained. DFT (M06-L/def2-TZVP/QZVP) suggests that BF_3/*trans*-$[(PPh_3)_2(CO)M(COCH_2Ph)]^+$ adduct formation is more favored for M = Pt than M = Pd. Natural bond orbital analysis shows that upon Lewis acid coordination, the acyl C−O bond is weakened, the natural charge of the acyl C is more positive, and the $\pi^*_{\text{acyl C−O}}$ orbital is lowered in energy relative to other unoccupied orbitals.

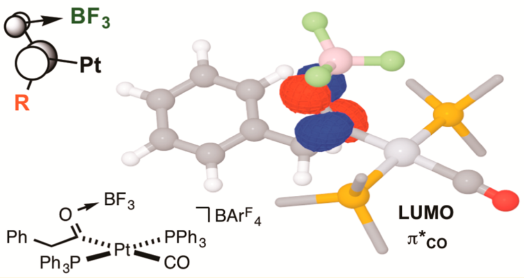

INTRODUCTION

Lewis acids promote metal-centered reactivity through ligand-based interactions with transition metal complexes,[1] such as facilitating migratory insertion of CO.[2] Shriver and co-workers established that Lewis acids can accelerate CO insertion into metal−carbon bonds and stabilize the resulting acyl complexes through association to the acyl oxygen.[3] Since Shriver's seminal work, only a handful of reports[4] address the thermodynamic stability of Lewis acid−acyl adducts. Moreover, Lewis acids are seldom added to transition-metal-catalyzed carbonylations,[5] despite the likelihood of acyl intermediates in these reactions.

A Lewis acid should increase acyl electrophilicity for the same reasons that Lewis acids influence organic carbonyl reactivity. Chart 1 shows illustrations comparing the LUMO of organic carbonyls and acyls.[6] Early metal η^2-acyls are highly electrophilic at the acyl carbon,[7] and Lewis acid O-coordination to η^1-acyl complexes should similarly polarize the acyl carbon and decrease the LUMO (π^*_{CO}) energy. Rare, *late* transition metal η^2-acyl complexes have reduced electrophilicity due to $d\pi/\pi^*_{CO}$ interactions.[7] However, such overlap is minimized in η^1 coordination shown in Chart 1, bottom.

Chart 1. LUMO Illustrations for Lewis Acid-Coordinated Ketones and Organotransition Metal Acyl Complexes

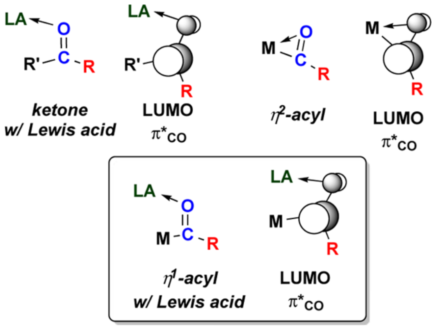

A lower LUMO energy could (a) make π^*_{CO} more available for reactions with exogenous nucleophiles and (b) promote internal attack by nucleophilic coligands, such as amines or alkyl ligands. The latter phenomenon resembles the accelerating effect of ligand−Lewis acid interactions on reductive elimination, for which there are both stoichiometric[8] and catalytic examples, such as hydrocyanation.[9]

We stress that this qualitative picture is based on an understanding of Lewis acid interactions with aldehydes and ketones. Shriver and co-workers[3] rationalized the C−O acyl bond lengthening of $CpFeL_2(COR)$ upon BF_3 binding as a resonance effect, shortening the M−C bond and increasing Fischer carbene character. Later theoretical work by Green and co-workers[10] provided a more nuanced picture: the HOMO and LUMO of iron acyls are both influenced by Lewis acid binding, with sigma and pi effects each contributing to lengthening of the C−O bond. Clearly the viewpoint in Chart 1 is insufficient to fully describe the variety of orbital interactions in organometallic settings.

Received: June 16, 2015

DOI: 10.1021/acs.organomet.5b00507

The present study aims to understand the bonding of Lewis acid−acyl adducts as a foundation for investigations of catalytic processes, much as previous studies[11] of Lewis acid−organic carbonyl adducts have led to improved catalysts. Our focus in this work is the chemistry of Pd and Pt acyl complexes, thought to be participants in various catalytic cycles, including hydroformylation[12] and carbonylation.[13] Evidence from experiment suggests a Pt acyl complex binds more strongly to Lewis acids than its Pd congener. This is reinforced by computational thermochemistry data and natural bond orbital (NBO) analysis.

■ RESULTS AND DISCUSSION

In Situ Preparation of Acyl Complexes. Yamamoto[13] and co-workers studied the mechanism of Pd-catalyzed carbonylation of benzyl chlorides by reacting cationic benzyl Pd and Pt complexes with CO to form acyl complexes in situ. **1a** ($[(PPh_3)_2Pt(CH_2Ph)][BAr^F{}_4]$; $BAr^F{}_4$ = tetrakis(3,5-bis(trifluoromethyl)phenyl)borate) and **1b** ($[(PPh_3)_2Pd(CH_2Ph)][BAr^F{}_4]$) (Chart 2) were prepared via abstraction of Cl^- from $(PPh_3)_2M(CH_2Ph)Cl$ using $NaBAr^F{}_4$ (see Experimental Section). The crystal structure obtained of **1b** is similar to η^3-benzyl complexes featuring bisphosphines (Xantphos, DPEphos, and DPPF) (see the Supporting Information).[14]

Chart 2. Cationic Benzyl Complexes $[(PPh_3)_2Pt(CH_2Ph)][BAr^F{}_4]$ (1a) and $[(PPh_3)_2Pd(CH_2Ph)][BAr^F{}_4]$ (1b)

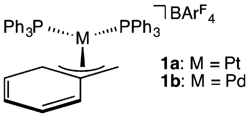

Treatment of **1a** with CO (1 atm) in CD_2Cl_2 (Scheme 1) forms a mixture of *trans*-$[(PPh_3)_2(CO)Pt(CH_2Ph)][BAr^F{}_4]$ (**2**) and acyl complex *trans*-$[(PPh_3)_2(CO)Pt(COCH_2Ph)][BAr^F{}_4]$ (**3**). Conversion to **3** is incomplete over several days at 1 atm CO. Since both are unstable outside of a CO atmosphere, the crude mixture of **2** and **3** was characterized via NMR spectroscopy under a CO atmosphere. A resonance at 2.95 ppm in the ^1H NMR spectrum (CD_2Cl_2, 298 K; Figure S5) is assigned to the CH_2 methylene protons of the (Pt-$COCH_2Ph$) moiety of **3**; the equivalent protons of **2** (Pt-CH_2Ph) are at 2.74 ppm. This downfield shift upon carbonylation is consistent with the behavior of analogous Pd complexes.[13] An HMBC experiment provides evidence for the proposed assignment (Figure S6). The ^1H NMR 2.95 ppm resonance exhibits coupling to a ^{13}C NMR signature at 224.62 ppm, consistent with the acyl CO of a cationic Pt(II) complex.[15] The *trans* configuration of **2** and **3** is confirmed by the presence of singlets, each with ^{195}Pt satellites, visible in the ^{31}P NMR spectrum (CD_2Cl_2, 298 K; 18.92 ppm, **2**; 13.12 ppm, **3**), as well as the triplet ^1H NMR coupling pattern of the benzyl protons of **2** ($^3J_{P,H}$ = 10.0 Hz).

Scheme 1. Reaction of $[(PPh_3)_2Pt(CH_2Ph)][BAr^F{}_4]$ (1a) with CO (1 atm)

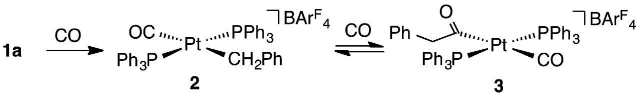

On the basis of the relative integrations of **2** and **3** (1.4:1 after several days at room temperature) and assuming [CO] = 0.024 M, estimated from the known solubility of CO in DCM[16] (mole fraction, 298 K, 1 atm = 1.54×10^{-3}; [DCM] = 15.62 M) the equilibrium constant for formation of **3** from **2** is K = 3.0×10 at 1 atm CO and 298 K. Therefore, $\Delta G° = -0.3$ kcal mol^{-1}.

A solution phase infrared spectrum of the above reaction mixture (1 atm CO, DCM) features a band at 2097 cm^{-1}, the only absorption in the range characteristic of cationic *trans*-platinum carbonyl complexes (2050−2150 cm^{-1}).[17] The ν_{CO} absorptions of either **2** or **3** may absorb at this frequency and potentially overlap. A broad band at 1609 cm^{-1} is presumably the carbonyl group of the acyl ligand of **3**. For comparison, Sen and co-workers[18] reported absorptions for *trans*-$[Pt(PPh_3)_2(CO)(COPh)]BF_4$ at 2070 cm^{-1} (terminal CO) and 1625 cm^{-1} (acyl CO), while Stang and co-workers[15] indicated absorptions at 2108 and 1658 cm^{-1} for *trans*-$[Pt(PPh_3)_2(CO)(\eta^1\text{-}(CO)(\text{methyl propanoate}))]OTf$ (a compound similarly unstable toward loss of CO).

Lewis Acids in Pt Carbonylation. When **1a** is reacted with 1 atm of CO in the presence of BF_3Et_2O (Scheme 2), the resonance for acyl complex **3** is shifted downfield, suggesting an interaction with BF_3; the chemical shifts of **2** are unchanged. Conversion of **2** to **3** is incomplete over several days. A downfield shift of acyl resonances upon Lewis acid complexation has been seen previously.[4d,19] At high concentrations of BF_3Et_2O relative to Pt, the peak is shifted as far as 3.05 ppm (Figure S7), while for [Pt] ≫ $[BF_3Et_2O]$ the peak does not shift appreciably (Figure S8).

Scheme 2. Proposed Coordination of BF_3 to *trans*-$[(PPh_3)_2(CO)Pt(COCH_2Ph)][BAr^F{}_4]$ (3)

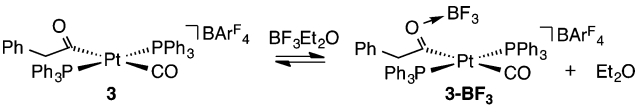

To assess the strength of Lewis acid−acyl binding, Stimson and Shriver previously determined Lewis acid−acyl equilibrium binding constants exclusively from quantitative IR studies,[20] while dynamic NMR studies underpin prior explorations of Lewis acid−carbonyl binding.[21] Two NMR-based approaches were used here to calculate thermodynamic parameters for BF_3 coordination to **3**. First, for a given concentration of BF_3Et_2O and **3**, the chemical shift of the diethyl ether methylene peak at room temperature (Figure S9) was established relative to free diethyl ether (3.43 ppm in DCM) and BF_3Et_2O (4.20 ppm). This approach, which assumes rapid exchange, was validated by Gajewski and Ngernmeesri for BF_3 complexation to carbonyl compounds,[22] and provides $\Delta G = 1.8 \pm 0.1$ kcal mol^{-1} at 293 K for the coordination of BF_3 to the acyl oxygen of **3**.

The BF_3 acyl complex is under slow exchange conditions at 253 K (Figure S9). Since both free Et_2O and complexed BF_3Et_2O resonances are observed, the relative integrations of the two peaks provide an equilibrium constant K = 0.1 at 253 K. A van't Hoff analysis (253−273 K; Table S1) provided thermodynamic parameters: $\Delta H° = -3.4 \pm 1.0$ kcal mol^{-1}, $\Delta S° = -0.018 \pm 0.100$ kcal mol^{-1} K^{-1}, $\Delta G° = 2.0 \pm 1.0$ kcal mol^{-1}.

The acyl oxygen's Lewis basicity can be estimated from the enthalpy of Lewis base−BF_3 binding in dichloromethane.[23] On the basis of this scale, the Pt acyl complex **3** has greater Lewis basicity ($-\Delta H°$ = 22.4 kcal mol^{-1}; see the Supporting

DOI: 10.1021/acs.organomet.5b00507

Table 1. Structural Parameters for 3, 3-bf3, 4, and 4-bf3 and Relevant X-ray Precedent

compound	M–C_{acyl}	M–P (av)	M–$C_{carbonyl}$	C=O (acyl)	C≡O (carbonyl)	C_{acyl}–M–$C_{carbonyl}$	Pt–C≡O
trans-$[Pt(COCO_2Me)(CO)(PPh_3)_2][BF_4]$[24]	2.04(1)	2.34	1.96(1)	1.18(2)	1.11(2)	176.6(6)	174.8(1)
trans-$[PtCl(COC_6H_{13})(PPh_3)_2]$[25]	2.02(1)	2.30		1.22(1)			
$[Pt(PNP)(COCH_2CH_3)]BF_4$[26]	2.002(10)	2.28		1.200(15)			
3 (computed)	2.082	2.383	1.978	1.205	1.137	175.55	172.49
3-bf3 (computed)	2.049	2.396	1.953	1.250	1.135	175.15	177.18
4 (computed)	2.060	2.403	2.031	1.196	1.134	176.06	172.64
4-bf3 (computed)	2.026	2.405	1.996	1.244	1.132	173.29	175.47

Information) than many functional groups, including nitriles (13–14 kcal mol^{-1}), aldehydes and ketones (16–19 kcal mol^{-1}), esters (14–18 kcal mol^{-1}), and ethers (18–22 kcal mol^{-1}), while most amines and amides are more Lewis basic than **3**.

Despite the exothermicity of Lewis acid binding, the reaction is endergonic at ambient temperature. Data obtained by Gajewski and Ngernmeesri[22] suggest that the entropy difference for the reaction of BF_3Et_2O with an aldehyde is negligible. Metal complex–BF_3 association might inhibit rotation of ligands on the Pt center or otherwise limit the dynamic behavior of **3**.

A side reaction forms toluene in varying amounts when **1a** is in the presence of Lewis acid, regardless of CO pressure. In the presence of protic solvent, Lewis acids generate Bronsted acids capable of Pt–C protonolysis,[27] the presumed mechanism here. Other mechanisms are conceivable,[28] but the present reaction requires Lewis acid. Attempts to slow or stop toluene formation by rigorous exclusion of water (silylation of glassware with bis(trimethylsilyl)acetamide,[29] drying solvents with various dessicants) failed. The rate and extent of this side reaction does not appear to influence the above binding data.

Other Lewis acids ($AlCl_3$, $B(C_6F_5)_3$) have similar effects on the reaction of **1a** with CO, but side reactions complicate analysis. With 20 equiv of $B(C_6F_5)_3$ added to **1a** (under 1 atm of CO) the acyl resonance shifts downfield (^1H NMR, CD_2Cl_2, 298 K, 3.05 ppm, $\Delta\delta$ 0.10), and the benzyl aromatic resonances shift upfield. Cooling the solution amplifies the effect (e.g., 253 K acyl resonance @ 3.15 ppm, $\Delta\delta$ 0.20). The resonance corresponding to **2** does not show temperature dependence. An enthalpically favored but entropically disfavored interaction between **3** and $B(C_6F_5)_3$ is consistent with the above. There is no spectroscopic evidence for $Ph_3P{:}B(C_6F_5)_3$,[30] but unassigned resonances (^1H NMR, 2.92 ppm; ^{31}P NMR, 8.27 ppm) are observed. Excess $AlCl_3$ causes an immediate color change from yellow to dark purple and an increase in the formation of toluene, as well as various other side products.

Lewis acid coordination to other sites, such as the O of the CO ligand or directly to the Pt(II)[31] center, may occur, but they have not been observed here. All NMR signals of Pt CO complex **2** are unaffected by BF_3, suggesting a lack of substantive interactions with carbonyl or Pt. Known reactions of BF_3[32] and $B(C_6F_5)_3$[27] with Pt(II) complexes occur without apparent Pt–B coordination. Another potential competing process, abstraction of PPh_3 by BF_3, should be apparent via ^{31}P NMR (CD_2Cl_2, 298 K: 11.8 ppm[33]), but no signal corresponding to $Ph_3P{:}BF_3$ was observed.

Pd Reaction. In contrast to the Pt congener, reaction of **1b** with 1 atm of CO does not result in immediate formation of an acyl complex. A single new species grows in by ^1H NMR (δ 3.32) over several days, presumably *trans*-$[(PPh_3)_2(CO)Pd(COCH_2Ph)][BAr^F{}_4]$ (**4**). IR spectroscopy on the sample was not attempted due to the very low concentration of acyl complex. With the addition of Lewis acids (BF_3Et_2O, $B(C_6F_5)_3$, $AlCl_3$) the conversion is more rapid, as expected.[3] Unlike the Pt complex **3**, the acyl chemical shift does not move appreciably upon addition of Lewis acid, precluding an estimation of binding strength by ^1H NMR. Toluene is again a side product when Lewis acids are used.

Computational Study. The coordination of Lewis acids to acyl complexes was investigated further using DFT. Calculations were performed using the M06-L functional[34] and Ahlrichs/Weigend basis functions (def2-TZVP/QZVP),[35] known to be an accurate, efficient method for evaluating organometallic thermochemistry.[36] The geometry-optimized structure of **3** (in dichloromethane via implicit SMD[37] solvation) demonstrates bond lengths and angles analogous to crystallographic data for similar structures (Table 1, Figure 1A).

Various structures of **3-BF$_3$** are possible depending on the site of BF_3 binding. Coordination to the acyl oxygen with B *cis* to Pt (Figure 1B) provided a stable minimum without

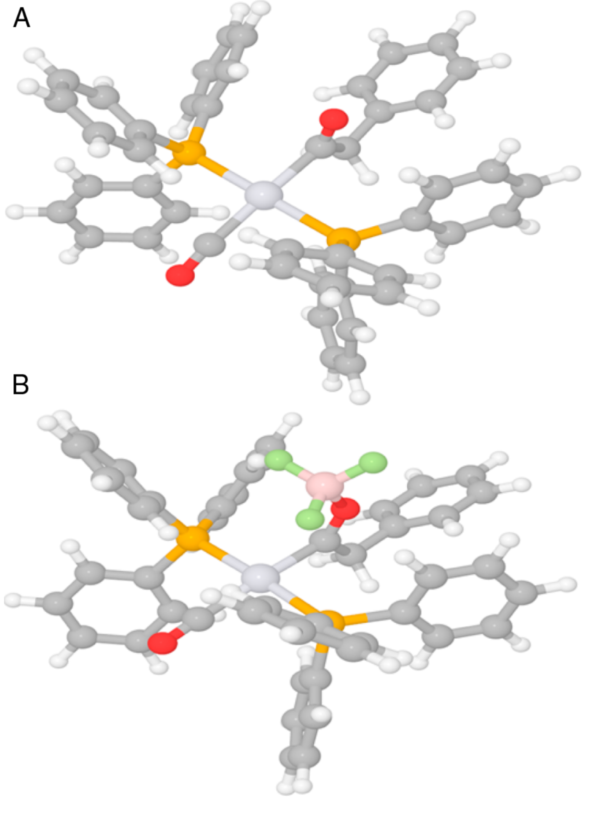

Figure 1. (A) Optimized DFT structure of **3**. (B) Optimized DFT structure of **3-bf3**.

constraints. Attempts to find optimized geometries for *trans* coordination to the acyl oxygen, Pt−B coordination (at an axial position), or BF_3 coordination to the oxygen atom of the carbon monoxide (carbonyl) ligand were unsuccessful, with Lewis acid coordination apparently disfavored relative to complete dissociation. Therefore, the following analysis was performed on the structure **3-bf3** shown in Figure 1B.

According to the structures of **3** and **3-bf3**, the largest changes in bond length upon BF_3 coordination are a lengthening of the acyl C−O bond (1.205 Å to 1.250 Å; Table 1) and a shortening of the Pt−C_{acyl} bond (2.082 Å to 2.049 Å). These changes mirror findings by Green and coworkers for the BF_3−$CpFeL_2(COR)$ system.[10] A decrease in the Pt−$C_{carbonyl}$ bond upon BF_3 binding suggests a weakening *trans* influence on coordination. The Pt−C≡O angle approaches linearity upon BF_3 binding. Optimized structures of the Pd congeners **4** and **4-bf3** show the same general trends.

To study the thermodynamics of the reaction of **3** with BF_3Et_2O, frequency calculations were performed on optimized structures of **3**, **3-bf3**, BF_3Et_2O, and BF_3. The difference in total electronic energy, ΔE, is −2.5 kcal mol^{-1}. The thermochemistry obtained via frequency calculations ($\Delta H° = -2.7$ kcal mol^{-1}, $\Delta S° = -0.005$ kcal mol^{-1} K^{-1}, $\Delta G° = -1.2$ kcal mol^{-1}) is reasonably consistent with experiment ($\Delta H° = -3.4$ kcal mol^{-1}, $\Delta S° = -0.018$ kcal mol^{-1} K^{-1}, $\Delta G° = 2.0$ kcal mol^{-1}; vide supra). Thermochemistry for the analogous reaction of **4** ($\Delta E = 0.6$ kcal/mol; $\Delta H° = 0.3$ kcal mol^{-1}, $\Delta S° = -0.005$ kcal mol^{-1} K^{-1}, $\Delta G° = 1.0$ kcal mol^{-1}) indicates that BF_3 coordination to the Pd congener **4** is less favorable.

To assist in understanding the influence of BF_3 on the orbitals of **3**, a natural bond orbital analysis (NBO 6.0) was performed on the computed structures of both **3** and **3-bf3**. In the following we discuss changes to the acyl ligand upon BF_3 binding using the carbon monoxide (carbonyl) ligand as reference. A natural population analysis (Table 2) shows that the charge on the acyl and carbonyl carbons increases upon Lewis acid coordination, while the charge on the oxygen of the acyl becomes more negative. For both **3** and **3-bf3**, the carbonyl carbon has a greater natural charge than the acyl carbon.

Table 2. Natural Population Analysis of 3 and 3-bf3

atom	natural charge		
	3	**3-bf3**	Δ
Pt	0.248	0.294	0.046
C (acyl)	0.397	0.431	0.034
C (carbonyl)	0.484	0.524	0.040
O (acyl)	−0.575	−0.598	−0.023
O (carbonyl)	−0.420	−0.402	0.018

The occupancy and energy for selected NBOs are shown in Table 3. The antibonding $\sigma^*_{acyl\ C-O}$ and $\pi^*_{acyl\ C-O}$ orbitals are stabilized by coordination of BF_3, their occupancy is increased, and the acyl antibonding orbitals become more polarized. Other orbitals, including those of the carbon monoxide ligand, are little changed by comparison. An energy level diagram (Figure 2) shows the influence of BF_3 on the acyl orbitals relative to the remainder of the metal complex. Effects on orbital energies are mostly localized to the acyl ligand, e.g., a lowering of $\pi^*_{acyl\ C-O}$ relative to $\pi^*_{carbonyl\ C-O}$. Figure 3 shows representative illustrations of preorthogonalized NBOs of **3-bf3**, which have the general shapes of organic carbonyl orbitals.

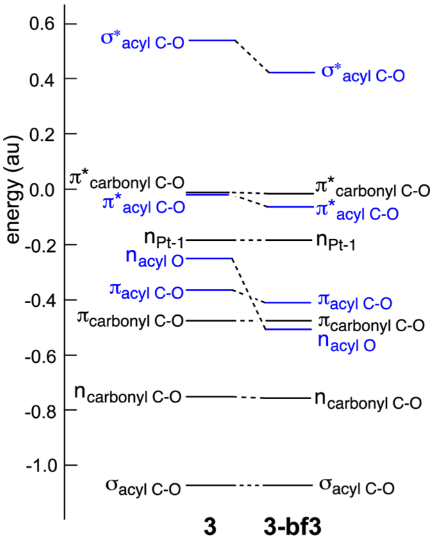

Figure 2. Energy level diagram (NBO) for **3** and **3-bf3**. Blue labels are used for orbitals on the acyl ligand. The n label refers to lone pairs; for example, n_{Pt-1} refers to the platinum lone-pair NBO with the highest energy.

As expected for a square planar complex,[38] two hyperbonds (three-center, four-electron bonds) are present in both **3** and **3-bf3**, each corresponding to mutually *trans* ligand pairs (Table

Table 3. Selected Natural Bond Orbitals (NBOs), Occupancies, and Energies

NBO	**3**		**3-bf3**	
	occupancy	energy (au)	occupancy	energy (au)
$\sigma_{acyl\ C-O}$	1.99	−1.075	1.99	−1.071
$\pi_{acyl\ C-O}$	1.98	−0.363	1.98	−0.408
$n_{acyl\ O}$	1.81	−0.250	1.67	−0.503
$\pi^*_{acyl\ C-O}$	0.12 (69.9% C, 30.1% O)	−0.014	0.19 (77.5% C, 22.5% O)	−0.064
$\sigma^*_{acyl\ C-O}$	0.022 (67.8% C, 32.2% O)	0.543	0.03 (70.3% C, 29.7% O)	0.430
$n_{carbonyl\ O}$	1.98	−0.752	1.98	−0.760
$\pi_{carbonyl\ C-O}$	2.00	−0.476	2.00	−0.479
$\pi^*_{carbonyl\ C-O}$	0.13	−0.011	0.14	−0.028
n_{Pt}	1.98	−0.172	1.98	−0.174
	1.95	−0.275	1.96	−0.290
	1.86	−0.271	1.86	−0.288
	1.83	−0.296	1.83	−0.314

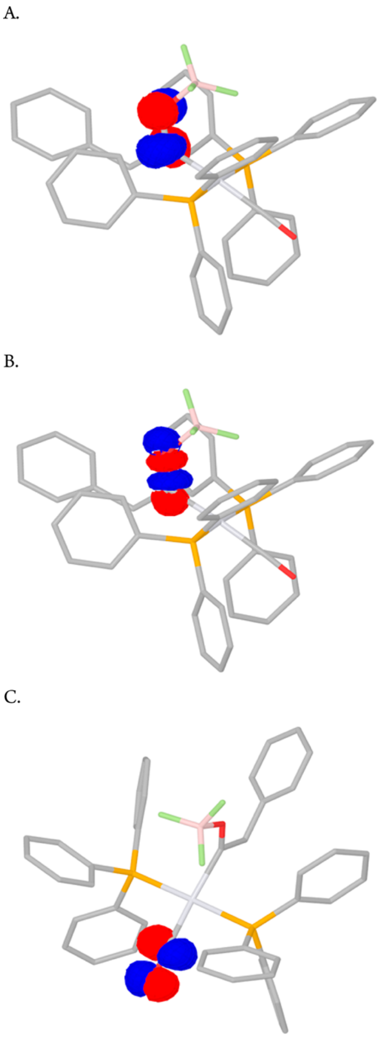

Figure 3. PNBOs of (A) $\pi^*_{\text{acyl C–O}}$; (B) $\sigma^*_{\text{acyl C–O}}$; and (C) $\pi^*_{\text{carbonyl C–O}}$ of **3-bf3**.

4). For the $\omega_{\text{C–Pt–C}}$ bond, the contribution from the Pt–C_{acyl} relative to a Pt–$C_{carbonyl}$ decreases from 58.3% in **3** to 55.3% in **3-bf3**. The contributions from each Pt–P (2c/2e) bond to the $\omega_{\text{P–Pt–P}}$ hyperbond remain equivalent on BF_3 coordination.

The acyl NBOs of **4** and **4-bf3** are qualitatively similar in energy and occupancy (Tables S2 and S3). The largest differences between the Pd and Pt systems are the reduced energy of the highest occupied n_M NBO (**4**, −0.225 au; **4-bf3**, −0.239 au) and the natural charges of C_{acyl} (**4**, 0.47; **4-bf3**, 0.48), O_{acyl} (**4**, −0.55; **4-bf3**, −0.60), and M (**4**, 0.27; **4-bf3**, 0.32).

Both experiment and computation support a metal dependence on Lewis acid–acyl binding affinity, but no simple explanation presents itself. Pt complex **3** and Pd complex **4** undergo similar bond length changes on BF_3 binding, and the NBO analysis of each is similar. The acyl O of **3** does have a more negative charge than that of **4**, suggesting a greater affinity for Lewis acids.

Pt acyl carbonyl compounds are known to undergo nucleophilic attack at the carbonyl rather than the acyl,[18,24] while selective Pd acyl attack is expected in carbonylation reactions.[13a] Comparing the natural charges of $C_{carbonyl}$ vs C_{acyl} in **3** and **4** yields a straightforward explanation. The Pt acyl carbon is much less positively charged than the Pt carbonyl and thus less prone to attack. Contrast this with the Pd acyl and carbonyl carbons, which have similar natural charges.

CONCLUSIONS

The present work shows the influence of Lewis acids on Pd and Pt organotransition metal acyl complexes. Changes in NBO energy and occupancy upon Lewis acid coordination support an increase in electrophilic character of the acyl ligand. Future studies will explore the influence of Lewis acids on acyl reactivity.

EXPERIMENTAL SECTION

General Methods. Unless otherwise specified, all manipulations were performed under a dry N_2 atmosphere using Schlenk techniques or a Vacuum Atmospheres inert atmosphere glovebox. Infrared spectra were collected using a Thermo Fisher Nicolet iS5 spectrometer with a sealed liquid cell (International Crystal Laboratories SL-3, 0.1 mm, CH_2Cl_2, 298 K). Analytical data were obtained from the CENTC Elemental Analysis Facility at the University of Rochester, funded by NSF CHE-0650456. NMR spectra were collected on Bruker Avance III 500 MHz and DRX 500 MHz instruments. ^{1}H NMR chemical shifts (δ, ppm) are referenced to residual protiosolvent resonances, and ^{13}C NMR chemical shifts are referenced to the deuterated solvent peak.[39] ^{31}P NMR chemical shifts are referenced using an 85% H_3PO_4 external standard (δ = 0). Dichloromethane, pentane, and toluene were purified using a commercial solvent purification system. Benzene, tetrahydrofuran, diethyl ether, and benzyl chloride were dried over a column of activated alumina and vacuum distilled. All deuterated NMR solvents (Cambridge Isotope Laboratories) were dried over activated 4 Å molecular sieves for 48 h before use. Sodium tetrakis(3,5-bistrifluoromethyl)phenylborate ($NaBAr^F_4$) was prepared using the procedure of Yakelis and Bergman.[40] Tris(pentafluorophenyl)borane ($B(C_6F_5)_3$) was purified via sublimation (100 mTorr, 90 °C) prior to use. Other chemicals were used as received from commercial suppliers. Carbon monoxide (Airgas, > 99.3% purity) was used directly as supplied.

***trans*-$(PPh_3)_2Pt(CH_2Ph)Cl$.** This known compound[41] was prepared in a one-pot, two-step sequence. $Pt(PPh_3)_4$ was synthesized from $K_2[PtCl_4]$ as previously reported[42] and, without purification, immediately treated with excess degassed benzyl chloride. After several hours of heating at 75 °C, the reaction flask was cooled to room temperature and the volatiles were removed in vacuo. The crude residue was extracted with toluene and filtered through Celite. The resulting solution was recrystallized from toluene/*n*-pentane. ^{1}H NMR (500 MHz, CD_2Cl_2): δ 7.62 (m, 12H, ArH), 7.42 (m, 6H, ArH), 7.36 (m, 12H, ArH), 6.80 (m, 1H, ArH), 6.70 (t, $^3J_{H,H}$ = 7.6 Hz, 2H, ArH), 6.40 (d, $^3J_{H,H}$ = 7.0 Hz, 2H, ArH), 2.27 (t, $^3J_{P,H}$ = 7.9 Hz, 2H, CH_2Ph). ^{31}P{^{1}H} NMR (202 MHz, CD_2Cl_2): δ 27.47 (s, $^1J_{Pt,P}$ = 1625 Hz).

$[(PPh_3)_2Pt(CH_2Ph)][BAr^F_4]$ (1a). To a 20 mL scintillation vial in the glovebox were added $(PPh_3)_2Pt(CH_2Ph)Cl$ (465 mg, 0.549 mmol), $NaBAr^F_4$ (495 mg, 0.559 mmol, 1.02 equiv), and DCM (10 mL). The mixture was allowed to stir for 48 h. After filtration through Celite, the solution was concentrated and transferred to a 4 mL vial. Layering the solution with *n*-pentane resulted in bright yellow crystals

Table 4. Hyperbonds in 3 and 3-bf3

hyperbond	3	3-bf3
$\omega_{\text{C–Pt–C}}$	58.3% Pt–C_{acyl}/41.7% Pt–$C_{carbonyl}$	55.3% Pt–C_{acyl}/44.7% Pt–$C_{carbonyl}$
$\omega_{\text{P–Pt–P}}$	49.7% Pt–P/50.3% Pt–P	49.8% Pt–P/50.2% Pt–P

DOI: 10.1021/acs.organomet.5b00507

over several days, which were dried in vacuo. Yield: 689 mg, 0.412 mmol, 75%; mp 179 °C. ^{1}H NMR (CD_2Cl_2, 500 MHz): δ 7.71 (s, 8H, BAr^F_4), 7.55 (s, 4H, BAr^F_4), 7.46–7.16 (m, 24H, ArH), 6.95–6.81 (m, 8H, ArH), 6.68 (t, $^3J_{H,H}$ = 7.6 Hz, 1H, *p*-CH_2*Ph*), 6.54 (d, $^3J_{H,H}$ = 6.8 Hz, 2H, *o*-CH_2*Ph*), 2.53 (m, 1H, C*H*$_2$Ph). $^{31}P\{^1H\}$ NMR (202 MHz, CD_2Cl_2): δ 24.01 (s, $^1J_{Pt,P}$ = 1660 Hz), 21.68 (s, $^1J_{Pt,P}$ = 2700 Hz). Anal. Calcd for $C_{75}H_{49}BF_{24}P_2Pt$: C, 53.81; H, 2.95. Found: C, 53.66; H, 2.89.

***trans*-$(PPh_3)_2Pd(CH_2Ph)Cl$.** This known compound[43] was prepared through a known procedure. To a yellow suspension of $Pd(PPh_3)_4$ (2.77 g, 2.40 mmol) in degassed benzene was added an excess of degassed benzyl chloride (10 mL) via cannula. After 30 min, the resulting dark yellow solution was reduced in vacuo. Diethyl ether (40 mL) was added to precipitate a yellow solid. Crude yield: 1.33 g, 1.76 mmol, 73%. Recrystallization from DCM/pentane provided yellow material with spectra consistent with literature values.[43]

$[(PPh_3)_2Pd(CH_2Ph)][BAr^F_4]$ (1b). To a 20 mL scintillation vial in the glovebox were added $(PPh_3)_2Pd(CH_2Ph)Cl$ (85 mg, 0.11 mmol), $NaBAr^F_4$ (99 mg, 0.11 mmol, 1.0 equiv), and DCM (3 mL). The mixture was allowed to stir for 2 h. After filtration through Celite, the solution was concentrated and transferred to a 4 mL vial. Layering the solution with toluene and cooling resulted in yellow-orange crystals, which were dried in vacuo and washed with toluene and pentane. Yield: 138 mg, 0.087 mmol, 79%; mp 136 °C (dec). ^{1}H NMR (500 MHz, CD_2Cl_2): δ 7.72 (s, 8H, BAr^F_4), 7.55 (s, 4H, BAr^F_4), 7.49–6.69 (m, 35H, ArH), 2.99 (t, $^3J_{P,H}$ = 4.4 Hz, 2H, C*H*$_2$Ph). ^{31}P NMR (202 MHz, CD_2Cl_2): δ 33.75 (s), 23.32 (s). Anal. Calcd for $C_{75}H_{49}BF_{24}P_2Pd$: C, 56.82; H, 3.12. Found: C, 56.56; H, 3.11.

Reaction of $[(PPh_3)_2Pt(CH_2Ph)][BAr^F_4]$ (1a) with 1 atm of CO. To a J. Young-style NMR tube were added 20 mg $[(PPh_3)_2Pt(CH_2Ph)][BAr^F_4]$ and 0.5 mL of DCM-d_2. The tube was attached to a Schlenk manifold, subjected to three freeze–pump–thaw cycles (in a liquid N_2 bath), backfilled with CO (1 atm), and sealed. The starting compound is immediately converted to *trans*-$[(PPh_3)_2(CO)Pt(CH_2Ph)][BAr^F_4]$ (**2**) and *trans*-$[(PPh_3)_2(CO)Pt(COCH_2Ph)][BAr^F_4]$ (**3**). The mixture of compounds cannot be purified or isolated due to facile loss of CO. *trans*-$[(PPh_3)_2(CO)Pt(CH_2Ph)][BAr^F_4]$ (**2**): ^{1}H NMR (CD_2Cl_2, 500 MHz) δ 2.74 (t, $^3J_{P,H}$ = 10.0 Hz, $^2J_{Pt,H}$ = 77.6 Hz); $^{31}P\{^1H\}$ NMR (CD_2Cl_2, 202 MHz) δ 18.92 (s, $^1J_{Pt,P}$ = 2740 Hz). *trans*-$[(PPh_3)_2(CO)Pt(COCH_2Ph)][BAr^F_4]$ (**3**): ^{1}H NMR (CD_2Cl_2, 500 MHz) δ 2.95 (s); $^{31}P\{^1H\}$ NMR δ 13.12 (s, $^1J_{Pt,P}$ = 3004 Hz).

Reaction of $[(PPh_3)_2Pd(CH_2Ph)][BAr^F_4]$ (1b) with 1 atm of CO. To a J. Young-style NMR tube were added 20 mg of $[(PPh_3)_2Pd(CH_2Ph)][BAr^F_4]$ and 0.5 mL of DCM-d_2. The tube was attached to a Schlenk manifold, subjected to three freeze–pump–thaw cycles (in a liquid N_2 bath), backfilled with CO (1 atm), and sealed. Over several days the starting compound forms trace *trans*-$[(PPh_3)_2(CO)Pd(COCH_2Ph)][BAr^F_4]$ (**4**): ^{1}H NMR (CD_2Cl_2, 500 MHz) δ 3.32 (s).

Computational Details. Density functional theory (DFT) calculations were performed using Gaussian 09, revision C.01 (keywords in parentheses below).[44] The M06-L functional[34] (m06l) and def2-TZVP[35] basis set (def2tzvp) were used for all nonmetal atoms, while the def2-QZVP[35] (qzvp) basis set was used for metals. The associated ECPs[45] were downloaded from the EMSL basis set exchange (http://bse.pnl.gov/).[46] Density fitting basis sets[47] were employed for all atoms (Denfit). All calculations were performed using the SMD solvation model of Truhlar and co-workers (scrf = smd, solvent = dichloromethane).[37] Justification of the above method for calculating organometallic thermochemistry is provided by Gusev,[36] who showed M06-L/TZVP/TZVPfit to be economical and accurate for this purpose.

Optimized geometries were obtained using tight convergence criteria (opt = tight) and an ultrafine grid (int = ultrafine). The optimized geometries were used in frequency calculations to ensure the absence of imaginary frequencies and to provide thermochemistry (enthalpy and free energy) values at 298.15 K and 1 atm. Natural bonding orbital calculations were performed using NBO version 6.0[48] in stand-alone GenNBO mode, using the NBO3 ARCHIVE (0.47) files generated from Gaussian 09 calculations.

■ ASSOCIATED CONTENT

Ⓢ Supporting Information

The Supporting Information is available free of charge on the ACS Publications website at DOI: 10.1021/acs.organomet.5b00507.

NMR spectra, computational thermochemistry, NBO analysis of **4** and **4-bf3**, and crystal structure report for $[(PPh_3)_2Pd(CH_2Ph)][BAr^F_4]$ (**1b**) (PDF)

Crystallographic Information File for $[(PPh_3)_2Pd(CH_2Ph)][BAr^F_4]$ (**1b**) (CIF)

Cartesian coordinates for all computed structures (XYZ)

■ AUTHOR INFORMATION

Corresponding Author

*E-mail: dob@temple.edu.

Notes

The authors declare no competing financial interest.

■ ACKNOWLEDGMENTS

This research was supported in part by the National Science Foundation through major research instrumentation grant number CNS-09-58854. We thank Boulder Scientific for a gift of $B(C_6F_5)_3$ and Dr. Charlie DeBrosse for performing and analyzing the HMBC NMR experiment. G.E.D. thanks Dr. Christine Hahn (Texas A&M–Kingsville) for helpful discussions.

■ REFERENCES

(1) Wang, C.; Xi, Z. *Chem. Soc. Rev.* **2007**, *36*, 1395–1406.

(2) Butts, S. B.; Holt, E. M.; Strauss, S. H.; Alcock, N. W.; Stimson, R. E.; Shriver, D. F. *J. Am. Chem. Soc.* **1979**, *101*, 5864–5866.

(3) Butts, S. B.; Strauss, S. H.; Holt, E. M.; Stimson, R. E.; Alcock, N. W.; Shriver, D. F. *J. Am. Chem. Soc.* **1980**, *102*, 5093–5100.

(4) (a) Miller, A. J. M.; Labinger, J. A.; Bercaw, J. E. *J. Am. Chem. Soc.* **2008**, *130*, 11874–11875. (b) Miller, A. J. M.; Labinger, J. A.; Bercaw, J. E. *Organometallics* **2010**, *29*, 4499–4516. (c) West, N. M.; Labinger, J. A.; Bercaw, J. E. *Organometallics* **2011**, *30*, 2690–2700. (d) Llewellyn, S. A.; Green, M. L. H.; Cowley, A. R. *Dalton Trans.* **2006**, 1776–1783.

(5) Williams, D. B. G.; Shaw, M. L.; Green, M. J.; Holzapfel, C. W. *Angew. Chem., Int. Ed.* **2008**, *47*, 560–563.

(6) Corcoran, R. C.; Ma, J. *J. Am. Chem. Soc.* **1992**, *114*, 4536–4542.

(7) Tatsumi, K.; Nakamura, A.; Hofmann, P.; Stauffert, P.; Hoffmann, R. *J. Am. Chem. Soc.* **1985**, *107*, 4440–4451.

(8) Liberman-Martin, A. L.; Bergman, R. G.; Tilley, T. D. *J. Am. Chem. Soc.* **2013**, *135*, 9612–9615.

(9) Shen, Q.; Hartwig, J. F. *J. Am. Chem. Soc.* **2007**, *129*, 7734–7735.

(10) Anderson, G. D. W.; Boys, O. J.; Cowley, A. R.; Green, J. C.; Green, M. L. H.; Llewellyn, S. A.; Maresca von Beckh, C.; Pascu, S. I.; Vei, I. C. *J. Organomet. Chem.* **2004**, *689*, 4407–4419.

(11) (a) Koito, Y.; Nakajima, K.; Kobayashi, H.; Hasegawa, R.; Kitano, M.; Hara, M. *Chem. - Eur. J.* **2014**, *20*, 8068–8075. (b) Hunt, I. R.; Rogers, C.; Woo, S.; Rauk, A.; Keay, B. A. *J. Am. Chem. Soc.* **1995**, *117*, 1049–1056. (c) Toyota, S.; Asakura, M.; Sakaue, T. *Bull. Chem. Soc. Jpn.* **2002**, *75*, 2667–2671. (d) Asao, N.; Asano, T.; Yamamoto, Y. *Angew. Chem., Int. Ed.* **2001**, *40*, 3206–3208. (e) Reetz, M. T.; Huellmann, M.; Massa, W.; Berger, S.; Rademacher, P.; Heymanns, P. *J. Am. Chem. Soc.* **1986**, *108*, 2405–2408.

(12) Vilches-Herrera, M.; Domke, L.; Börner, A. *ACS Catal.* **2014**, *4*, 1706–1724.

(13) (a) Lin, Y.-S.; Yamamoto, A. *Organometallics* **1998**, *17*, 3466–3478. (b) Lin, Y.-S.; Yamamoto, A. *Bull. Chem. Soc. Jpn.* **1998**, *71*, 723–734.

(14) Johns, A. M.; Utsunomiya, M.; Incarvito, C. D.; Hartwig, J. F. *J. Am. Chem. Soc.* **2006**, *128*, 1828–1839.

(15) Hinkle, R. J.; Stang, P. J.; Arif, A. M. *Organometallics* **1993**, *12*, 3510−3516.

(16) Magee, M. P.; Li, H.-Q.; Morgan, O.; Hersh, W. H. *Dalton Trans.* **2003**, 387−394.

(17) (a) Cherwinski, W. J.; Clark, H. C. *Inorg. Chem.* **1971**, *10*, 2263−2267. (b) Kubota, M.; Rothrock, R. K.; Geibel, J. *J. Chem. Soc., Dalton Trans.* **1973**, 1267−1269.

(18) Sen, A.; Chen, J. T.; Vetter, W. M.; Whittle, R. R. *J. Am. Chem. Soc.* **1987**, *109*, 148−156.

(19) Smeltz, J. L.; Lilly, C. P.; Boyle, P. D.; Ison, E. A. *J. Am. Chem. Soc.* **2013**, *135*, 9433−9441.

(20) Stimson, R. E.; Shriver, D. F. *Inorg. Chem.* **1980**, *19*, 1141−1145.

(21) (a) Hartman, J. S.; Stilbs, P.; Forsén, S. *Tetrahedron Lett.* **1975**, *16*, 3497−3500. (b) Gillespie, R. J.; Hartman, J. S. *Can. J. Chem.* **1968**, *46*, 2147−2157. (c) Fratiello, A.; Onak, T. P.; Schuster, R. E. *J. Am. Chem. Soc.* **1968**, *90*, 1194−1198.

(22) Gajewski, J. J.; Ngernmeesri, P. *Org. Lett.* **2000**, *2*, 2813−2815.

(23) Maria, P. C.; Gal, J. F. *J. Phys. Chem.* **1985**, *89*, 1296−1304.

(24) Huang, T. M.; You, Y. J.; Yang, C. S.; Tzeng, W. H.; Chen, J. T.; Cheng, M. C.; Wang, Y. *Organometallics* **1991**, *10*, 1020−1026.

(25) Bardi, R.; Piazzesi, A. M.; Del Pra, A.; Cavinato, G.; Toniolo, L. *J. Organomet. Chem.* **1982**, *234*, 107−115.

(26) Carlisle, S.; Matta, A.; Valles, H.; Bracken, J. B.; Miranda, M.; Yoo, J.; Hahn, C. *Organometallics* **2011**, *30*, 6446−6457.

(27) Heyduk, A. F.; Labinger, J. A.; Bercaw, J. E. *J. Am. Chem. Soc.* **2003**, *125*, 6366−6367.

(28) Milstein, D.; Stille, J. K. *J. Org. Chem.* **1979**, *44*, 1613−1618.

(29) Hughes, R. P.; Rose, P. R.; Rheingold, A. L. *Organometallics* **1993**, *12*, 3109−3117.

(30) Stapleton, R. L.; Chai, J.; Taylor, N. J.; Collins, S. *Organometallics* **2006**, *25*, 2514−2524.

(31) Hodali, H. A. *J. Chem. Eng. Data* **1987**, *32*, 382−383.

(32) Beaulieu, W. B.; Rauchfuss, T. B.; Roundhill, D. M. *Inorg. Chem.* **1975**, *14*, 1732−1734.

(33) Lehman, D. D.; Shriver, D. F. *Inorg. Chem.* **1974**, *13*, 2203−2207.

(34) Zhao, Y.; Truhlar, D. G. *J. Chem. Phys.* **2006**, *125*, 194101.

(35) Weigend, F.; Ahlrichs, R. *Phys. Chem. Chem. Phys.* **2005**, *7*, 3297−3305.

(36) Gusev, D. G. *Organometallics* **2013**, *32*, 4239−4243.

(37) Marenich, A. V.; Cramer, C. J.; Truhlar, D. G. *J. Phys. Chem. B* **2009**, *113*, 6378−6396.

(38) Glendening, E. D.; Landis, C. R.; Weinhold, F. *WIREs Comput. Mol. Sci.* **2012**, *2*, 1−42.

(39) Fulmer, G. R.; Miller, A. J. M.; Sherden, N. H.; Gottlieb, H. E.; Nudelman, A.; Stoltz, B. M.; Bercaw, J. E.; Goldberg, K. I. *Organometallics* **2010**, *29*, 2176−2179.

(40) Yakelis, N. A.; Bergman, R. G. *Organometallics* **2005**, *24*, 3579−3581.

(41) (a) Yamamoto, Y.; Yamazaki, H. *Bull. Chem. Soc. Jpn.* **1971**, *44*, 1873−1875. (b) Strukul, G.; Michelin, R. A.; Orbell, J. D.; Randaccio, L. *Inorg. Chem.* **1983**, *22*, 3706−3713.

(42) Ugo, R.; Cariati, F.; Monica, G. L.; Mrowca, J. J. Tris- and Tetrakis(Triphenylphosphine)-Platinum(0). In *Inorganic Syntheses*; John Wiley & Sons, Inc.: New York, 1990; Vol. *28*, pp 123−126.

(43) Fitton, P.; McKeon, J. E.; Ream, B. C. *J. Chem. Soc. D* **1969**, 370−371.

(44) Frisch, M. J.; Trucks, G. W.; Schlegel, H. B.; Scuseria, G. E.; Robb, M. A.; Cheeseman, J. R.; Scalmani, G.; Barone, V.; Mennucci, B.; Petersson, G. A.; Nakatsuji, H.; Caricato, M.; Li, X.; Hratchian, H. P.; Izmaylov, A. F.; Bloino, J.; Zheng, G.; Sonnenberg, J. L.; Hada, M.; Ehara, M.; Toyota, K.; Fukuda, R.; Hasegawa, J.; Ishida, M.; Nakajima, T.; Honda, Y.; Kitao, O.; Nakai, H.; Vreven, T.; Montgomery, J. A., Jr.; Peralta, J. E.; Ogliaro, F.; Bearpark, M. J.; Heyd, J.; Brothers, E. N.; Kudin, K. N.; Staroverov, V. N.; Kobayashi, R.; Normand, J.; Raghavachari, K.; Rendell, A. P.; Burant, J. C.; Iyengar, S. S.; Tomasi, J.; Cossi, M.; Rega, N.; Millam, N. J.; Klene, M.; Knox, J. E.; Cross, J. B.; Bakken, V.; Adamo, C.; Jaramillo, J.; Gomperts, R.; Stratmann, R. E.; Yazyev, O.; Austin, A. J.; Cammi, R.; Pomelli, C.; Ochterski, J. W.; Martin, R. L.; Morokuma, K.; Zakrzewski, V. G.; Voth, G. A.; Salvador, P.; Dannenberg, J. J.; Dapprich, S.; Daniels, A. D.; Farkas, Ö.; Foresman, J. B.; Ortiz, J. V.; Cioslowski, J.; Fox, D. J. *Gaussian 09*; Gaussian, Inc.: Wallingford, CT, USA, 2009.

(45) Andrae, D.; Häußermann, U.; Dolg, M.; Stoll, H.; Preuß, H. *Theor. Chim. Acta* **1990**, *77*, 123−141.

(46) Schuchardt, K. L.; Didier, B. T.; Elsethagen, T.; Sun, L.; Gurumoorthi, V.; Chase, J.; Li, J.; Windus, T. L. *J. Chem. Inf. Model.* **2007**, *47*, 1045−1052.

(47) Weigend, F. *Phys. Chem. Chem. Phys.* **2006**, *8*, 1057−1065.

(48) Glendening, E. D.; Badenhoop, J. K.; Reed, A. E.; Carpenter, J. E.; Bohmann, J. A.; Morales, C. M.; Landis, C. R.; Weinhold, F. *NBO 6.0*; Theoretical Chemistry Institute, University of Wisconsin: Madison, WI, USA, 2013.

DOI: 10.1021/acs.organomet.5b00507